Diffraction grating with suppressed zero order fabricated using dielectric forces

Gary G. Wells,[1] Naresh Sampara,[1] Emmanouil E. Kriezis,[2] John Fyson,[3] and Carl V. Brown[1,*]

[1]*School of Science and Technology, Nottingham Trent University, Clifton Lane, Nottingham NG11 8NS, UK*

[2]*Aristotle University of Thessaloniki, Department of Electrical & Computer Engineering, Thessaloniki GR 54 124, Greece*

[3]*Wolfson Centre for Materials Processing, Brunel University, Uxbridge, Middlesex UB8 3PH, UK*

**Corresponding author: carl.brown@ntu.ac.uk*

Received July 26, 2011; revised October 12, 2011; accepted October 13, 2011;
posted October 14, 2011 (Doc. ID 151757); published November 15, 2011

An electric-field-assisted method to produce diffractive optical devices is demonstrated. A uniform film of liquid UV curable resin was produced as a drying ring from an organic solvent. Dielectrophoresis forces maintained the stability of the thin film and also imprinted a periodic corrugation deformation of pitch 20 μm on the film surface. Continuous *in situ* voltage-controlled adjustment of the optical diffraction pattern was carried out simultaneously with UV curing. A fully cured solid phase grating was produced with the particular voltage-selected tailored optical property that the zero transmitted order was suppressed for laser light at 633 nm. © 2011 Optical Society of America

OCIS codes: 050.1950, 160.4670.

The use of electric-field assistance in the fabrication of polymer devices and optical components is attractive because complex patterns, structures, and morphologies can be self-assembled starting from relatively simple geometries. Submicrometer polymer patterning, accurate molds, and novel optical devices have previously been created from a thin film of polymer melt in a capacitor structure [1–5]. Orthogonal electric-field geometries and electrowetting on dielectric have also been used with UV curing of resin droplets to determine the shapes of millimeter-scale lenses [6–8]. In-plane electric-field geometries have been used to pattern polymer surfaces and to induce phase separation with applications in optical display fabrication [9–14]. We have previously shown how dielectrophoresis forces [15,16] can controllably wrinkle the surfaces of dielectric liquids [17,18]. In this work, a periodic wrinkle is created on a film of UV curable liquid resin and *in situ* voltage-controlled adjustment of the optical diffraction pattern during UV curing of the resin creates the final solid phase grating.

The experimental device, Fig. 1, consisted of an array of parallel interdigital coplanar transparent indium tin oxide stripe electrodes, shown by the black rectangles, on a glass substrate. The electro-optical layer was created by dispensing a 10 ± 1 μL droplet of UV curable resin (NOA65, Norland Products, New Jersey, USA) dissolved in acetone, 10% by weight. The acetone evaporates within 60 s of dispensing the droplet, which was confirmed for larger droplets using a mass balance. This resulted in a stable "drying ring" spread liquid resin layer, typically with diameter between 14 and 16 mm, central thickness in the range of 2 to 3 μm, and thickness variation of less than ± 0.5 μm over the 5 mm $\times$ 5 mm electrode area.

Applying a 10 kHz square-wave voltage of peak amplitude V_o to each alternate electrode finger (with interposed electrodes at earth potential) produces a periodic corrugation, or "wrinkle," at the resin/air interface. The wrinkle is created because dielectrophoresis forces collect the polarizable resin liquid in the vicinity of the gaps between the electrodes where the fringing electric fields are highly nonuniform, which, in turn, removes liquid from the regions immediately above the electrode fingers [15–17]. Since dielectrophoresis forces are polarity independent, the period p of the corrugation is equal to the electrode period, i.e., $p = 20$ μm for an electrode width (which equals the electrode gap) of 10 μm.

The device was mounted horizontally and illuminated in transmission with laser light of wavelength 633 nm polarized perpendicular to the corrugation direction. The one-dimensional periodic change in the thickness of the transparent resin layer creates a one-dimensional spatially periodic modulation of the optical path. This acts as a phase grating, which diffracts the transmitted laser light for which the amplitude of the grating, and thus the intensities of the diffracted orders, can be tuned by adjusting the voltage applied to the electrodes. Figure 2 shows the quasi-static experimental intensities of the 0 (circles), +1 (plus symbols), and +2 (cross symbols) transmitted diffracted orders while the voltage V_o (10 kHz square wave) was increased at a slow rate of 0.2 V/s. Data is shown for a surface corrugation of pitch $p = 20$ μm.

The intensities of the diffracted orders vary between maxima and minima as a function of voltage. Intuitively, this arises because the phase difference between a ray traveling through a peak in the wrinkle and a ray traveling through an adjacent trough (mapped to the angular direction of a particular diffracted order) passes through destructive and constructive interference conditions in

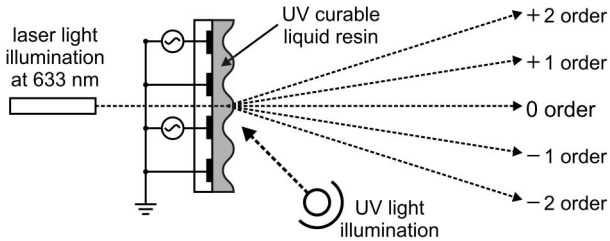

Fig. 1. Experimental geometry. A film of liquid UV curable resin coats a structured transparent electrode on glass. Applying a voltage creates a periodic deformation in the surface of the film, which diffracts laser light.

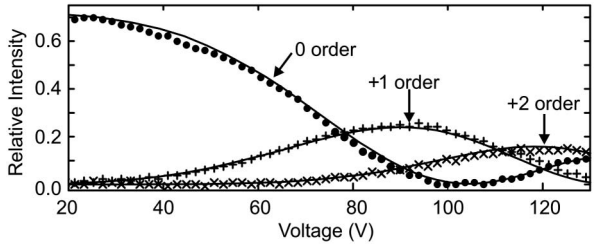

Fig. 2. Intensity of the zero (circles), +1 (plus symbols), and +2 diffracted (crosses) orders as a fraction of total incident intensity of laser light at 633 nm transmitted through the liquid resin film with a surface corrugation of pitch 20 μm versus the applied voltage V_o (10 kHz square wave). The solid curves show the theoretical predictions using the FDTD method.

turn as the peak-to-peak amplitude A of the wrinkle increases monotonically as a function of the increasing voltage V_o. In reality, the observed amplitudes of diffracted intensities at a given voltage are determined not simply by the grating depth but by the precise shape of the periodic surface profile at that voltage [19].

Having shown that the diffraction pattern from the liquid resin can be voltage tuned, the next stage is UV curing *in situ* with the voltage applied to create a solid permanent grating structure. Figure 3 shows the first diffracted order intensity for a wrinkle on a resin layer that was continuously illuminated at 45° to the layer normal by an 8 W UV lamp (T5 UV fluorescent tube, Philips Lighting, Netherlands) placed 60 mm from the device while an amplitude modulated 10 kHz driving voltage was applied. The voltage amplitude alternated discontinuously between 90 V (starting at $t = 0$ s) and 10 V every 30 s, as shown at the top of the figure.

The first diffracted order intensity rises sharply after $t = 0$ s, which is associated with the wrinkle amplitude A increasing from zero toward a value determined by the applied voltage. At $t = 30$ s, the voltage is abruptly reduced and the intensity decreases, associated with the wrinkle amplitude decaying back toward zero. In subsequent cycles, the amplitude of the peak-to-peak intensity response and also the gradient of the response

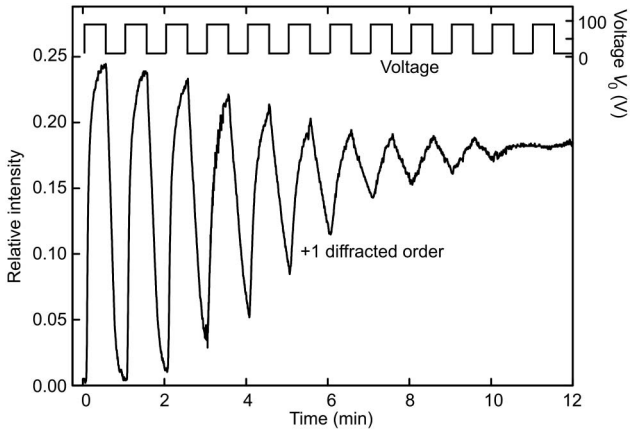

Fig. 3. Fractional intensity of laser light diffracted into the +1 order (lower plot, left-hand axis) is shown while the device was addressed by a 10 kHz voltage square-wave waveform $V_o(t)$ that was amplitude modulated by a slow 1/60 Hz square wave (upper plot, right hand axis). The resin was simultaneously cured by exposure to continuous UV illumination from an 8 W UV lamp.

after each sudden change in voltage both decrease significantly. The increase of the viscosity of UV curable resin during UV illumination [20,21] means that the wrinkle amplitude becomes progressively less responsive to changes in the voltage as curing progresses. After 720 s, there is very little change in the diffracted intensity within each cycle, which can be associated with the wrinkle amplitude A settling toward a fixed value.

Figure 4 shows diffraction pattern intensity versus angle scans from a solid grating with pitch 20 μm that was fabricated with the particular voltage preselected optical property that the zero-order transmitted intensity of laser light at 633 nm wavelength was minimized and suppressed. A voltage of $V_o = 105 \pm 1$ V was applied initially to the liquid resin layer to minimize the zero order. When the UV illumination was applied, the voltage was continually adjusted to maintain the zero order at its lowest intensity. In practice, this necessitated an increase in the voltage by 15 V during the first 10 min of curing. After 30 min, the grating was fully cured and solidified. The surface profile measured using a stylus contact profiler (Dektak 6M, Veeco, New York, USA) is shown inset in Fig. 4. The average layer thickness and peak-to-peak surface grating amplitude values were $h = 2.23\,\mu$m and $A = 0.81\,\mu$m, respectively.

The diffraction efficiency $\eta(n)$ of the nth diffracted order can be defined as $100 \times I(n)/I_o$, where $I(n)$ is the integrated intensity in the nth order and I_o is the total intensity of incident laser light. In the center of the 5 mm × 5 mm electrode area, which was illuminated during the feedback-optimization procedure, $\eta(0) = 0.6\%$ and $\eta(+1) = 20.5\%$. At eight positions symmetrically around the center, all 2 mm from the edges of the electrode area, diffraction efficiencies were measured in the range $\eta(0) = 0.8\%$ and $\eta(+1) = 20.9\%$, to $\eta(0) = 2.2\%$ and $\eta(+1) = 21.2\%$. These variations were due to thickness variations across the liquid resin film. The polarization sensitivity was negligible, for example, in the center of the grating $\eta(+1) = 20.5 \pm 0.1\%$ for laser illumination polarized perpendicular to the corrugation direction compared to $\eta(+1) = 20.6 \pm 0.1\%$ for polarization parallel to the corrugation direction.

The open circles in Fig. 4 show the theoretical predictions of finite-difference time-domain (FDTD)-based optical simulations [22,23] calculated directly from the four periods of the measured surface profile shown in Fig. 4 and assuming a refractive index of 1.524 for the fully cured resin [24]. The FDTD method accounts for the detailed shape of the resin surface and rigorously consid-

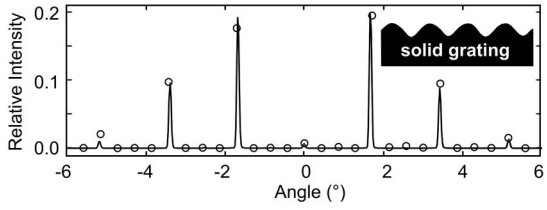

Fig. 4. Diffracted intensity as a fraction of total incident intensity (solid curve) versus angle for transmission of laser light at 633 nm through a fully cured solid transparent grating of pitch 20 μm for which the actual surface profile, measured using a stylus contact profiler, is shown in the inset. The circles show the theoretical predictions of FDTD optical simulations.

ers light diffraction without introducing any approximations apart from numerical discretization. The measured surface profile in Fig. 4 was also used in the FDTD simulations to produce theoretical values for the intensity transmitted into the zero, +1, and +2 diffracted orders, shown as the solid curves in Fig. 2. The peak-to-peak amplitude of the resin/grating surface was scaled in relation to the voltage with the function $A = \alpha[V_o]^2$, while the shape of the profile was kept constant [18]. The theoretical curve in Fig. 2 was obtained with the value $\alpha = (7.41 \pm 0.05) \times 10^{-11}\,\mathrm{m\,V^{-2}}$. The agreement between the theoretical simulations and the experimental results in Figs. 2 and 4 is very good considering that the only other fitting parameter is the optical loss, which was set at 30% for the solid gratings and 20% for the liquid gratings. Slight asymmetries in the calculated diffraction efficiencies between positive and negative orders and the low amplitude components of the shape at the longer pitch of 40 μm (between the orders at 20 μm) predicted by the FDTD calculations are due to the small asymmetries and differences observed between neighboring periods in the surface profile inset in Fig. 4. The measurements show less asymmetry and show negligible intensities of the intermediate orders since the laser beam samples an extended device area, resulting in an averaging effect.

In conclusion, we have shown a new electric-field-assisted approach to producing solid optical devices with micrometer-scale features for which the optical properties are voltage preselected when the optical medium is in its liquid phase. As an example, we have shown how continuous adjustment of the voltage during UV curing can produce a solid grating with suppressed intensity of the transmitted zero order. The grating contained 250 periods covering 5 mm. Dielectric-force-assisted spreading of the liquid resin can potentially produce much wider gratings (giving higher resolution), provided that thickness uniformity is maintained, for example, by initially dispensing a more dilute solution of resin in acetone.

Our approach suggests a potential manufacturing technique in which an automated optical-intensity–voltage-feedback control loop is used to create a device with particular optical properties. Any changes in refractive index, volume (and thus grating shape), surface tension, and dielectric constant of the UV curable resin during the curing process would be compensated for [21]. A simple phase diffraction grating has been demonstrated, but the techniques could be extended to one- or two-dimensional arrays of independently addressable elements. This would allow solid zone plate or holographic wavefront modulation devices with optimized efficiencies to be produced using an automated process. The same principles could also apply with more complex electrode geometries to the creation of light collection or concentration optical components in devices (e.g., for solar cells or three-dimensional stereoscopic displays), where it may be possible to make use of a preexisting electrode microstructure.

We gratefully acknowledge Prof. Glen McHale, Dr. Michael Newton, and Dr. David Fairhurst for stimulating discussions. N. Sampara gratefully acknowledges studentship funding from Nottingham Trent University.

References

1. E. Schäffer, T. Thurn-Albrecht, T. P. Russell, and U. Steiner, Nature **403**, 874 (2000).
2. M. D. Morariu, N. E. Voicu, E. Schäffer, Z. Lin, and T. P. Russell, Nat. Mater. **2**, 48 (2003).
3. G. Jin and G. Kim, Langmuir **27**, 828 (2011).
4. A. J. Das and K. S. Narayan, Opt. Lett. **34**, 3391 (2009).
5. R. V. Craster and O. K. Matar, Rev. Mod. Phys. **81**, 1131 (2009).
6. S. Yang, T. N. Krupenkin, P. Mach, and E. A. Chandross, Adv. Mater. **15**, 940 (2003).
7. F. T. O'Neill, G. Owen, and J. T. Sheridan, Optik **116**, 158 (2005).
8. Z. Zhan, K. Wang, H. Yao, and Z. Cao, Appl. Opt. **48**, 4375 (2009).
9. D. Salac, W. Lu, C.-W. Wang, and A. M. Sastry, Appl. Phys. Lett. **85**, 1161 (2004).
10. K. Amundson, E. Helfand, D. D. Davis, X. Qian, S. S. Patel, and S. D. Smith, Macromolecules **24**, 6546 (1991).
11. C.-H. Wang, P. Chen, and C.-Y. D. Lu, Phys. Rev. E **81**, 061501 (2010).
12. Y. Kim, J. Francl, B. Taheri, and J. L. West, Appl. Phys. Lett. **72**, 2253 (1998).
13. A. E. Büyüktanir, N. Gheorghiu, J. L. West, M. Mitrokhin, B. Holter, and A. Glushchenko, Appl. Phys. Lett. **88**, 031101 (2006).
14. H. Ren, S.-T. Wu, and Y.-H. Lin, Phys. Rev. Lett. **100**, 117801 (2008).
15. H. A. Pohl, *Dielectrophoresis: The Behaviour of Neutral Matter in Non-Uniform Electric Fields*, Cambridge Monographs on Physics (Cambridge University, 1978).
16. T. B. Jones, M. Gunji, M. Washizu, and M. J. Feldman, J. Appl. Phys. **89**, 1441 (2001).
17. C. V. Brown, G. G. Wells, M. I. Newton, and G. McHale, Nat. Photon. **3**, 403 (2009).
18. C. V. Brown, W. Al-Shabib, G. G. Wells, G. McHale, and M. I. Newton, Appl. Phys. Lett. **97**, 242904 (2010).
19. J. W. Goodman, *Introduction to Fourier Optics*, 2nd ed. (McGraw-Hill, 1996).
20. Y. Otsubo, T. Amari, and K. Watanabe, J. Appl. Polym. Sci. **31**, 323 (1986).
21. S. Radhakrishnan and R. A. Pethrick, J. Appl. Polymer Sci. **51**, 863 (1994).
22. A. Taflove, Wave Motion **10**, 547 (1988).
23. E. E. Kriezis and S. J. Elston, Opt. Commun. **177**, 69 (2000).
24. J.-H. Park and I. C. Khoo, Appl. Phys. Lett. **87**, 091110 (2005).